How to cite: *Angew. Chem. Int. Ed.* **2022,** *61,* e202214145
International Edition: doi.org/10.1002/anie.202214145
German Edition: doi.org/10.1002/ange.202214145

Electrocatalytic Cyanide Reduction

Overcoming Electrostatic Interaction via Strong Complexation for Highly Selective Reduction of CN^- into N_2

Lei Tian, Long-Shuai Zhang, Ling-Ling Zheng, Ying Chen, Lin Ding, Jie-Ping Fan, Dai-She Wu, Jian-Ping Zou, and Sheng-Lian Luo*

Abstract: Limited by the electrostatic interaction, the oxidation reaction of cations at the anode and the reduction reaction of anions at the cathode in the electrocatalytic system nearly cannot be achieved. This study proposes a novel strategy to overcome electrostatic interaction via strong complexation, realizing the electrocatalytic reduction of cyanide (CN^-) at the cathode and then converting the generated reduction products into nitrogen (N_2) at the anode. Theoretical calculations and experimental results confirm that the polarization of the transition metal oxide cathodes under the electric field causes the strong chemisorption between CN^- and cathode, inducing the preferential enrichment of CN^- to the cathode. CN^- is hydrogenated by atomic hydrogen at the cathode to methylamine/ammonia, which are further oxidized into N_2 by free chlorine derived from the anode. This paper provides a new idea for realizing the unconventional and unrealizable reactions in the electrocatalytic system.

Electrocatalytic (EC) systems are widely applied in environmental contaminant control and fuel conversion.[1] The direct/indirect redox reactions in EC systems dominantly occur at the solid–liquid interface between the electrode and the solvent.[2] Benefitting from the electrostatic interaction, inorganic ions can be efficiently enriched on the electrode surface and the derivative redox reactions occur.[3] However, electrostatic interaction is a double-edged sword. The anodic oxidation of cations and cathodic reduction of anions are severely inhibited by electrostatic repulsion.[4]

At present, the above difficulties in the EC systems can be preliminarily resolved through the following three strategies: 1) Regulating the existent form of ions;[5] 2) Modifying electrodes to enhance the combination with ions;[6] 3) Constructing novel reactors (such as H-type double cell).[7] However, there are many drawbacks still existed in these strategies. The binding ability between the targeted electrodes and ions is not strong to get rid of the electrostatic interaction. Besides, though the electrostatic interaction can be weakened by separating anode and cathode chambers in the new reactors, the isolated redox reactions make it hard to realize the high-selective conversion of ions.[8] Taking anions such as cyanides (CN^-) for example, under the electric field, these anions induced by electrostatic interaction will preferentially enrich at the anode and are oxidized to cyanates (CNO^-).[9] Subject to the alkaline nature of the CN^- solution, the hydrolysis of CNO^- into ammonia (NH_3/NH_4^+) cannot happen, thereby inhibiting the conversion of CN^- into nitrogen (N_2).[10] Therefore, to efficiently realize the selective conversion of CN^- to N_2, it is vital to design a strategy to immensely enhance the binding ability between CN^- and the cathode, and to efficiently overcome the electrostatic attraction from the anode.

Herein, a novel strategy is proposed to overcome electrostatic interaction and further realize the selective conversion of CN^- into N_2 in the EC system. The transition metal oxides (TMOs) are used as the cathodes because the polarization of the transition metal oxides cathodes under an electric field can cause a strong complexation between transition metals and CN^-, resulting in the enhanced enrichment of CN^-. Then, CN^- is hydrogenated at the cathode, and the electrocatalytic reduction products are further oxidized into N_2 by the free chlorine, which is derived from the activation of NaCl electrolyte by the dimensionally stable anode (DSA, Ti/RuO_2-IrO_2). The mechanisms of enrichment and selective conversion are well elaborately investigated through experiments and theoretical calculations. Finally, the potential application of the EC system is investigated by treating the practical cyanide-containing wastewater. This paper provides a new idea for the cathodic reduction of anions or anodic oxidation of cations in the EC system and develops a new synergetic conversion mechanism for the highly efficient and selective conversion of CN^- into N_2 for the first time.

Three transition metal oxides (NiO, Fe_2O_3 and Co_3O_4) are selected as the cathodes, and the adsorption energy (E_{ads}) between the cathodes and CN^- with or without the input of voltage is analyzed by theoretical calculations. As shown in Figures 1a, S2, and S3, with the voltage input (−1.1 V vs RHE), the binding ability of CN^- with three transition metal oxide cathodes is significantly promoted,

[*] L. Tian, Dr. L.-S. Zhang, L.-L. Zheng, Y. Chen, Dr. L. Ding, Prof. J.-P. Zou, Prof. S.-L. Luo
National-Local Joint Engineering Research Center of Heavy Metals Pollutants Control and Resource Utilization
Nanchang Hangkong University
Nanchang, Jiangxi 330063 (P. R. China)
E-mail: zjp_112@126.com

L. Tian, L.-L. Zheng, Y. Chen, Prof. J.-P. Fan, Prof. D.-S. Wu, Prof. J.-P. Zou
Key Laboratory of Poyang Lake Environment and Resource Utilization, Ministry of Education, School of Resources & Environment, Nanchang University
Nanchang, Jiangxi 330031 (P. R. China)

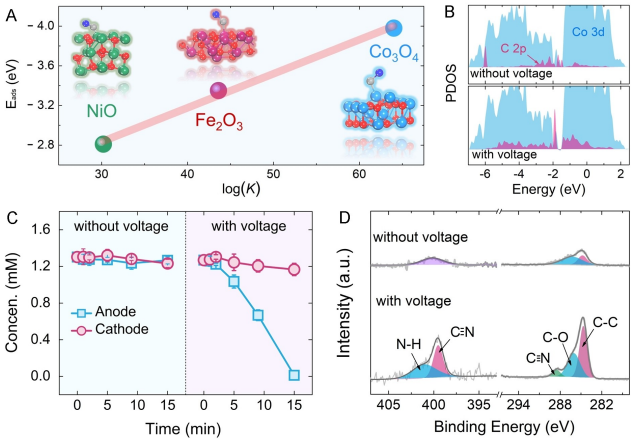

Figure 1. a) Adsorption energy between Co_3O_4, Fe_2O_3 and NiO cathodes and CN^- with voltage input; b) Density of states spectrum of CN^- and Co_3O_4 with or without voltage input; c) Concentration change of CN^- between the anode and Co_3O_4 cathode districts with or without voltage input; and d) XPS spectra of C1s and N1s of Co_3O_4 cathode with or without voltage input.

and E_{ads} between the TMOs cathodes and CN^- will linearly increase with the increase of the complex stability constant between the metals and CN^-. The binding ability between Co_3O_4 cathode and CN^- (−3.98 eV) is stronger than that of Fe_2O_3 (−3.35 eV, log$K$ = 43.6) and NiO (−2.81 eV, log$K$ = 30.2) cathodes due to the higher complex stability constant between Co and CN^- (log$K$ = 64.0). The density of states (DOS) spectrum demonstrates that the overlap areas between C 2p and Co 3d are increased after the voltage input (Figure 1b), indicating that the interaction between CN^- and Co_3O_4 cathode is enhanced and the charge migration between Co_3O_4 and CN^- occurs. As a result, the binding of CN^- and Co_3O_4 cathode is converted from the original physisorption to chemisorption, forming metal-cyanide bonds.

As shown in Figures 1c and S4, all cathodes show no obvious adsorption performance for CN^-. In absence of voltage, CN^- is distributed uniformly in the EC system and there is no concentration gradient between the cathode and anode districts. However, with the input of voltage (−1.1 V vs RHE), the concentration of CN^- in the anode district decreases significantly from 1.35 mM to 0.11 mM within 15 min, while the concentration of CN^- in the Co_3O_4 cathode district invariably remains at a high level (around 1.30 mM). A huge concentration gradient between the anode and Co_3O_4 cathode districts is observed, which is more significant than that of Fe_2O_3 and NiO cathodes (Figures S5 and S6). Due to the strong interaction between the TMOs cathodes and CN^-, the dynamic mass transfer of CN^- from the anode district to the cathode district and from the solution to the cathode interface occurs, resulting in the CN^- concentration in the cathode district much higher than that in the anode district. This phenomenon is different from that with the traditional active carbon fiber (ACF) and fluorine-doped tin oxide (FTO) as the cathodes (Figures S7 and S8). In addition, there are characteristic peaks of C≡N bonds in C1s and N1s of XPS spectra of Co_3O_4 cathode after the input of voltage, and some peaks (such as N–H, C–C) of intermediates are observed (Figures 1d).[11] These results confirm that the mass transfer of CN^- to the Co_3O_4 cathode is realized with the input of voltage because the interaction between CN^- and the cathode can conquer the electrostatic attraction from the DSA anode.

Five kinds of cathodes are used in the EC system to investigate the effects of different enrichment directions on the selective conversion of CN^- into N_2. As demonstrated in Figure 2a and Table S1, when ACF and FTO are used as the cathodes, the conversion of CN^- into N_2 is merely 7.6 % and 2.1 %, respectively. Since there is no special interaction between CN^- and ACF/FTO cathode,[12] CN^- is enriched at the anode induced by the electrostatic attraction, resulting in that CN^- merely oxidized into CNO^- and can not be efficiently converted into N_2. As a comparison, when the transition metal oxides are used as the cathodes, the selective conversion of CN^- into N_2 is markedly promoted and increases with the increase of the binding capacity between CN^- and cathodes (Figure S9). Nearly 100 % of CN^- can be converted into N_2 when Co_3O_4 is used as the cathode, much superior to the cathodes of Fe_2O_3 (78.4 %) and NiO (43.1 %). The efficient enrichment of CN^- at the cathode can significantly promote the selective conversion of CN^- into N_2.

Besides, the concentration variation of products in the EC system with different electrolytes is further monitored to explore the synergistic effect between the DSA anode and the Co_3O_4 cathode. As shown in Figures 2b, S10, and S11, when Na_2SO_4 is used as the electrolyte, about 57 % of CN^- is converted and the dominant products of CN^- in the EC system are NH_3 and CH_3NH_2. The concentrations of NH_3 and CH_3NH_2 increase to 0.62 mM and 0.13 mM within 6 h,

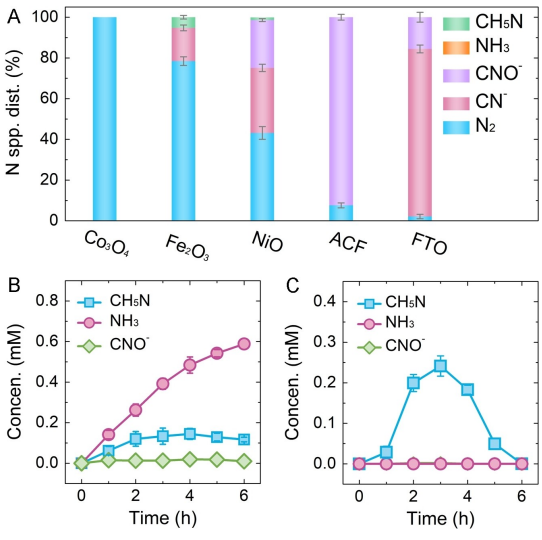

Figure 2. a) Distribution of nitrogen species with different cathodes and NaCl electrolyte after 6 h reaction; b) Concentration variation of intermediates with Co_3O_4 cathode and Na_2SO_4 electrolyte; and c) Concentration variation of intermediates with Co_3O_4 cathode and NaCl electrolyte.

respectively. Under the circumstances, no oxidizing active species are existing in the EC system, and the formation of NH_3 and CH_3NH_2 does not derive from the hydrolysis of CNO^- and the reduction of N_2 (Figures S12 and S13). As a result, CN^- is merely reduced at the Co_3O_4 cathode and the formed reduction products can not be further oxidized. For comparison, when NaCl is used as the electrolyte, nearly 100 % of CN^- is converted and only CH_3NH_2 is detected during the conversion process. The concentration of CH_3NH_2 reaches a maximum of 0.24 mM at 3 h and gradually decreases to 0 mM (Figures 2c and S14). Because Cl^- can be activated into active chlorine species at the DSA anode, the generated reduction products (NH_3 and CH_3NH_2) can be further oxidized into N_2 by active chlorine species.[13] The efficient oxidation of the reduction products in the solution enables the reduction products on the cathode interface to rapidly diffuse into the solution, thereby exposing more active sites and further promoting the rapid conversion of CN^-. Based on the above results, it is found that the synergy of the cathode and anode can effectively realize the selective conversion of CN^- into N_2 when NaCl is used as the electrolyte.

The cyclic voltammetry (CV) curve illustrates that there is a distinct peak in the range of −1.0 to −2.0 V in the absence of CN^-, which is attributed to the formation of H_2.[14] However, the peak disappears in presence of CN^- (Figure 3a), resulting from that CN^- can effectively react with atomic hydrogen (H*) at the Co_3O_4 cathode to prevent the self-quenching of H*, thereby inhibiting the formation of H_2.[15] Besides, the conversion performance of CN^- in the EC system is restrained after the addition of tert-butanol (a scavenger for H*), and there are characteristic peaks of H*-addition products in the electron spin resonance (ESR) spectra (Figures 3b and 3c),[16] further indicating that H* plays a vital role in the conversion of CN^-.

The reduction mechanism of CN^- at the Co_3O_4 cathode is further analyzed by theoretical calculation. As demonstrated in Figures S15 and S16, the adsorption of CN^- on the Co_3O_4 cathode is the rate-limiting step during the whole reduction process. Because the energy barrier for CN^- adsorption at Co atoms in octahedrons (0.69 eV) is much lower than that in tetrahedrons (1.13 eV) (Figure 3d), Co atoms in octahedrons are the main active sites for CN^- reduction. Besides, H* is the dominating reduction species and it is derived from the decomposition of H_2O at O atoms in Co_3O_4 because the energy barrier for H_2O activation into H* at O atoms is much lower than that at Co atoms (Figure S17). The reduction mechanism of CN^- at the Co_3O_4 cathode is shown in Equations (1)–(10). Since the CH_2NH_2* intermediates are more prone to the cleavage of C–N bonds (Figure 3e), CN^- is mainly reduced to NH_3 and CH_4 at the Co_3O_4 cathode, which is consistent with the results in Figure 2c. The generated CH_4 is detected by gas chromatography (Figure S18 and Table S2). In conclusion, when the Co_3O_4 is used as the cathode, CN^- can be efficiently hydrogenated by H* to form NH_3/CH_4 (major) and CH_3NH_2 (minor) in the EC system.

$$CN^- \rightarrow CN^* \quad (1)$$

$$H_2O + e^- \rightarrow H^* + OH^- \quad (2)$$

$$CN^* + H^* \rightarrow CHN^* \quad (3)$$

$$CHN^* + H^* \rightarrow CHNH^* \quad (4)$$

$$CHNH^* + H^* \rightarrow CH_2NH^* \quad (5)$$

$$CH_2NH^* + H^* \rightarrow CH_2NH_2{}^* \quad (6)$$

$$CH_2NH_2{}^* + H^* \rightarrow CH_3NH_2 \quad (7)$$

$$CH_2NH_2{}^* + H^* \rightarrow CH_3{}^* + NH_2{}^* \quad (8)$$

$$CH_3{}^* + H^* \rightarrow CH_4 \quad (9)$$

$$NH_2{}^* + H^* \rightarrow NH_3 \quad (10)$$

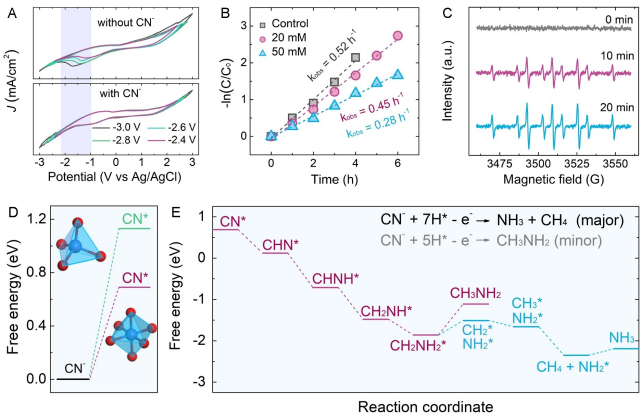

Figure 3. a) Cyclic voltammetry curve of EC system with or without CN^-; b) Conversion of CN^- with the addition of tert-butanol; c) ESR spectra of H* in the EC system; d) Energy barrier of rate-limiting step of CN^- reduction at Co atoms in octahedron or tetrahedron; and e) Optimal reaction path of CN^- at the Co_3O_4 cathode (reactive site at Co in octahedron).

The as-formed NH_3 and CH_3NH_2 can be further oxidized into N_2 by the oxidizing species (such as free chlorine, $Cl^•$, $ClO^•$, $Cl_2^{•-}$, and ClO^-) in the EC system, which are derived from the activation of Cl^- by the DSA anode.[17] Therefore, the oxidative species during the CN^- conversion process are explored by using NH_3/CH_3NH_2 as the model reactants and CBZ as the scavenger for $HO^•$, $Cl^•$, $ClO^•$, and $Cl_2^{•-}$ ($kHO^•$, CBZ = 8.8×10^9 $M^{-1}s^{-1}$, $kCl^•$, CBZ = 3.3×10^{10} $M^{-1}s^{-1}$, $kClO^•$, CBZ = 1.97×10^8 $M^{-1}s^{-1}$, and $kCl_2^{•-}$, CBZ = 4.3×10^7 $M^{-1}s^{-1}$).[18] As shown in Figures S19 and S20, the conversion of NH_3 and CH_3NH_2 is not inhibited in presence of CBZ, indicating that $HO^•$, $Cl^•$, $ClO^•$, and $Cl_2^{•-}$ are not dedicated to the oxidation of NH_3 and CH_3NH_2. The only oxidative species should be free chlorine (ClO^-, p*Ka*(HClO/ClO^-) = 7.54), which can efficiently and selectively oxidize NH_3 and CH_3NH_2 into N_2 [Eqs. (11)–(14)].

Based on the above results, the conversion path of CN^- in the EC system can be summarized. Benefitting from the strong binding ability between CN^- and Co_3O_4 cathode,

CN^- is preferentially enriched at the cathode and is hydrogenated by H* to generate NH_3 and CH_3NH_2. Subsequently, NH_3 and CH_3NH_2 are further oxidized to N_2 by free chlorine derived from the DSA anode. The overcoming of electrostatic attraction and the synergy of the cathode and anode can effectively realize the selective conversion of CN^- into N_2.

$$2Cl^- - 2e^- \rightarrow Cl_2 \quad (11)$$

$$Cl_2 + 2OH^- \rightarrow ClO^- + Cl^- + H_2O \quad (12)$$

$$2CH_3NH_2 + 9ClO^- \rightarrow N_2\uparrow + 2CO_2\uparrow + 5H_2O + 9Cl^- \quad (13)$$

$$2NH_3 + 3ClO^- \rightarrow N_2\uparrow + 3H_2O + 3Cl^- \quad (14)$$

Five cycle experiments are carried out to investigate the stability of the EC system. As shown in Figure 4a, a negligible inhibition of the conversion of CN^- into N_2 is observed after five cycles. Besides, the morphology and structure of the Co_3O_4 cathode after five cycles are consistent with that before the reaction, and the leaching concentration of cobalt ions after each cycle is negligible (Figures 4b, 4c, S21, and S22). These results confirm that the EC system has excellent stability. In addition, 16.07 mM of CN^- in the practical cyanide-containing wastewater can be efficiently converted within 18 h and 82.8 % of total nitrogen (TN) is removed within 22 h in the EC system (Figure 4d). Because the residual TN concentration is close to the concentration difference between the initial TN and CN^- (Table S3), about 100 % of CN^- in the practical cyanide-containing wastewater is selectively converted into N_2, which is much superior to the conversion of CN^- with ACF cathode (Figure 4e). The EC system constructed in this study has outstanding feasibility for the treatment of practical cyanide-containing wastewater.

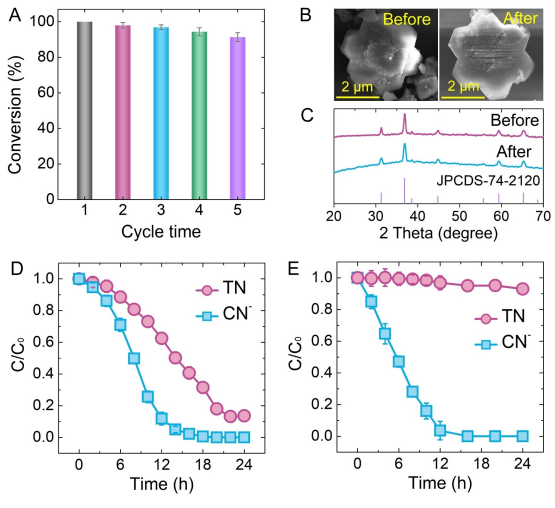

Figure 4. a) Conversion of CN^- into N_2 with 5 cycles; b) SEM images of Co_3O_4 before and after 5 cycles; c) XRD spectrum of Co_3O_4 before and after 5 cycles; d) Treatment of practical cyanide-containing wastewater with Co_3O_4 cathode; and e) Treatment of practical cyanide-containing wastewater with ACF cathode.

Subject to the electrostatic interaction and the derived semi-reactions, CN^- cannot be selectively converted into N_2 in traditional EC systems. In this study, a novel strategy is proposed to overcome the electrostatic interaction in the EC system, regulating the direction of enrichment and utilizing the synergy of anode and cathode for the selective conversion of CN^- into N_2. Noteworthily, under the electric field, a strong chemisorption interaction can be generated between the TMOs cathode and CN^-, which can overcome the electrostatic attraction of the anode, leading to the preferential enrichment of CN^- to the cathode. CN^- is preferentially hydrogenated to NH_3 and CH_3NH_2 by H*, and the as-formed NH_3 and CH_3NH_2 are further converted into N_2 by free chlorine derived from the DSA anode. Finally, the EC system exhibits excellent applicability for the treatment of practical cyanide-containing wastewater. This paper provides a new idea for the realization of the cathodic reduction of anions or anodic oxidation of cations and opens a new avenue to realize the highly efficient and selective conversion of CN^- into N_2.

Acknowledgements

We gratefully acknowledge the financial support of the National Natural Science Foundation of China (52170082, 51878325, 51938007, and 52100186), the National Key R&D Program of China (2018YFC1902002), and the Natural Science Foundation of Jiangxi Province (20212ACB203008).

Conflict of Interest

The authors declare no conflict of interest.

Data Availability Statement

The data that support the findings of this study are available from the corresponding author upon reasonable request.

Keywords: Cyanide · Electrocatalytic System · Electrostatic Interaction · Hydrogenation · Nitrogen

[1] a) D. Bohra, I. Ledezma-Yanez, G. N. Li, W. de Jong, E. A. Pidko, W. A. Smith, *Angew. Chem. Int. Ed.* **2019**, *58*, 1345–1349; *Angew. Chem.* **2019**, *131*, 1359–1363; b) D. Kim, S. Yu, F. Zheng, I. Roh, Y. F. Li, S. Louisia, Z. Y. Qi, G. A. Somorjai, H. Frei, L. W. Wang, P. D. Yang, *Nat. Energy* **2020**, *5*, 1032–1042; c) J. L. Wang, H. Y. Tan, Y. P. Zhu, H. Chu, H. M. Chen, *Angew. Chem. Int. Ed.* **2021**, *60*, 17254–174267; *Angew. Chem.* **2021**, *133*, 17394–17407; d) Z. X. Tao, C. L. Rooney, Y. Y. Liang, H. L. Wang, *J. Am. Chem. Soc.* **2021**, *143*, 19630–19642.
[2] a) C. Long, J. Y. Han, J. Guo, C. Y. Yang, S. Q. Liu, Z. Y. Tang, *Chem Catalysis* **2021**, *1*, 509–522; b) S. J. Shin, D. H. Kim, G. Bae, S. Ringe, H. Choi, H. K. Lim, C. H. Choi, H. Kim, *Nat. Commun.* **2022**, *13*, 172; c) P. Chen, Y. Mu, L. Tian,

X. H. Jiang, J. P. Zou, S. L. Luo, *Chemosphere* **2022**, *291*, 132817; d) H. Sheng, A. N. Jans, R. D. Ross, D. Kaiman, J. Huang, B. Song, J. R. Schmidt, S. Jin, *Energy Environ. Sci.* **2020**, *13*, 4189–4203.

[3] a) Y. H. Liu, H. J. Jiang, Z. H. Hou, *Angew. Chem. Int. Ed.* **2021**, *60*, 11133–11137; *Angew. Chem.* **2021**, *133*, 11233–11237; b) C. Choi, G. H. Gu, J. Noh, H. S. Park, Y. Jung, *Nat. Commun.* **2021**, *12*, 4353.

[4] a) L. Wei, D. J. Liu, B. A. Rosales, J. W. Evans, J. Vela, *ACS Catal.* **2020**, *10*, 3618–3628; b) J. Crawford, H. Q. Yin, A. J. Du, A. P. O'Mullane, *Angew. Chem. Int. Ed.* **2022**, *61*, e20221604; *Angew. Chem.* **2022**, *134*, e20221604; c) Y. T. Wang, H. J. Li, W. Zhou, X. Zhang, B. Zhang, Y. F. Yu, *Angew. Chem. Int. Ed.* **2022**, *61*, e202202604; *Angew. Chem.* **2022**, *134*, e202202604.

[5] a) M. L. Zhu, Y. Yang, S. B. Xi, C. Z. Diao, Z. G. Yu, W. S. V. Lee, J. M. Xue, *Small* **2021**, *17*, 2005616; b) H. Y. Liu, H. M. C. Lant, J. L. Troiano, G. F. Hu, B. Q. Mercado, R. H. Crabtree, G. W. Brudvig, *J. Am. Chem. Soc.* **2022**, *144*, 8449–8453.

[6] a) M. Van den Bergh, A. Krajnc, G. Mali, D. E. De Vos, *Angew. Chem. Int. Ed.* **2020**, *59*, 14086–14090; *Angew. Chem.* **2020**, *132*, 14190–14194; b) J. Z. Cai, B. L. Niu, Q. H. Xie, N. Lu, S. Y. Huang, G. H. Zhao, *Environ. Sci. Technol.* **2022**, *56*, 2917–2935; c) N. M. Mahmoodi, M. Oveisi, A. Taghizadeh, M. Taghizadeh, *J. Hazard. Mater.* **2019**, *368*, 746–759.

[7] a) J. P. Zou, Y. Chen, S. S. Liu, Q. J. Xing, W. H. Dong, X. B. Luo, W. L. Dai, X. Xiao, J. M. Luo, J. Crittenden, *Water Res.* **2019**, *150*, 330–339; b) D. L. Guo, Y. B. Liu, H. D. Ji, C. C. Wang, B. Chen, C. S. Shen, F. Li, Y. X. Wang, P. Lu, W. Liu, *Environ. Sci. Technol.* **2021**, *55*, 4045–4053; c) Z. C. Liu, G. Zhang, H. C. Lan, H. J. Liu, J. H. Qiu, *Environ. Sci. Technol.* **2021**, *55*, 12596–12606.

[8] a) S. Garcia-Segura, M. Lanzarini-Lopes, K. Hristovski, P. Westerhoff, *Appl. Catal. B* **2018**, *236*, 546–568; b) X. Li, W. Q. Fan, Y. J. Bai, Y. Liu, F. F. Wang, H. Y. Bai, W. D. Shi, *Chem. Eng. J.* **2022**, *433*, 133225; c) Y. T. Wang, H. J. Li, W. Zhou, X. Zhang, B. Zhang, Y. F. Yu, *Angew. Chem. Int. Ed.* **2022**, *61*, e202202604; *Angew. Chem.* **2022**, *134*, e202202604.

[9] a) X. Zhao, J. J. Zhang, J. H. Qu, *Electrochim. Acta* **2015**, *180*, 129–137; b) F. Y. Chen, C. Z. Hu, M. Sun, H. J. Liu, J. H. Qu, Z. Y. Tao, *Chem. Eng. J.* **2017**, *330*, 1187–1194; c) F. J. Qi, B. Yang, Y. B. Wang, R. Mao, X. Zhao, *ACS Sustainable Chem. Eng.* **2017**, *5*, 5001–5007.

[10] a) W. K. Teo, T. C. Tan, *Water Res.* **1987**, *21*, 677–682; b) L. Tian, P. Chen, X. H. Jiang, L. S. Chen, L. L. Tong, H. Y. Yang, J. P. Fan, D. S. Wu, J. P. Zou, S. L. Luo, *Water Res.* **2022**, *209*, 117890; c) X. Zhao, J. J. Zhang, M. Qiao, H. J. Liu, J. H. Qiu, *Environ. Sci. Technol.* **2015**, *49*, 4567–4574; d) M. S. Koo, H. Kim, K. E. Lee, W. Choi, *ACS ES&T Eng.* **2021**, *1*, 228–238.

[11] T. Nakayama, K. Inamura, Y. Inoue, S. Ikeda, K. Kishi, *Surf. Sci.* **1987**, *179*, 47–58.

[12] a) S. C. Tian, T. B. Li, H. B. Zeng, W. Guan, Y. Wang, X. Zhao, *J. Colloid Interface Sci.* **2016**, *482*, 205–211; b) S. C. Tian, Y. B. Li, X. Zhao, *Electrochim. Acta* **2015**, *180*, 746–755.

[13] a) Y. Zhang, J. H. Li, J. Bai, L. S. Li, S. Chen, T. S. Zhou, J. C. Wang, L. G. Xia, Q. J. Xu, B. X. Zhou, *Environ. Sci. Technol.* **2019**, *53*, 6945–6953; b) Y. Zhang, X. Y. Huang, J. H. Li, J. Bai, C. H. Zhou, L. Li, J. C. Wang, M. C. Long, X. Y. Zhu, B. X. Zhou, *Environ. Sci. Technol.* **2022**, *56*, 9693–9701.

[14] a) Z. M. Lou, J. Xu, J. S. Zhou, K. L. Yang, Z. Cao, Y. Z. Li, Y. L. Liu, L. P. Lou, X. H. Xu, *Chem. Eng. J.* **2019**, *374*, 211–220; b) Y. J. Zhou, G. Zhang, Q. H. Ji, W. Zhang, J. Y. Zhang, H. J. Liu, J. H. Qiu, *Environ. Sci. Technol.* **2019**, *53*, 11383–11390.

[15] Y. M. Shi, B. Zhang, *Chem. Soc. Rev.* **2016**, *45*, 1529.

[16] a) H. B. Zeng, G. Zhang, Q. H. Ji, H. J. Liu, X. Hua, H. L. Xia, M. Sillanpää, J. H. Qu, *Environ. Sci. Technol.* **2020**, *54*, 14725–14731; b) D. H. Huang, D. J. Kim, K. Rigby, X. C. Zhou, X. H. Wu, A. Meese, J. F. Niu, E. Stavitski, J. H. Kim, *Environ. Sci. Technol.* **2021**, *55*, 13306–13316.

[17] a) C. R. Costa, C. M. R. Botta, E. L. G. Espindola, P. Olivi, *J. Hazard. Mater.* **2008**, *153*, 616–627; b) D. Dionisio, L. H. E. Santos, M. A. Rodrigo, A. J. Motheo, *Electrochim. Acta* **2020**, *338*, 135901.

[18] a) K. Guo, Z. Wu, S. Yan, B. Yao, W. Song, Z. Hua, X. Zhang, X. Kong, X. Li, J. Y. Fang, *Water Res.* **2018**, *147*, 184–194; b) L. Tian, S. S. Liu, X. H. Jiang, L. S. Chen, S. L. Wu, W. J. Xiao, J. P. Fan, D. S. Wu, J. P. Zou, *Sci. Total Environ.* **2021**, *782*, 146857; c) L. Tian, M. Zhu, L. S. Zhang, L. J. Zhou, J. P. Fan, D. S. Wu, J. P. Zou, *J. Environ. Chem. Eng.* **2022**, *10*, 107414; d) L. S. Zhang, X. H. Jiang, Z. A. Zhong, L. Tian, Q. Sun, Y. T. Cui, X. Lu, J. P. Zou, S. L. Luo, *Angew. Chem. Int. Ed.* **2021**, *60*, 21751–21755; *Angew. Chem.* **2021**, *133*, 21919–21923.

Manuscript received: September 25, 2022
Accepted manuscript online: October 17, 2022
Version of record online: November 15, 2022